Available online at www.sciencedirect.com
SCIENCE DIRECT®
Journal of Sound and Vibration 286 (2005) 697–727
JOURNAL OF SOUND AND VIBRATION
www.elsevier.com/locate/jsvi

Control of internal resonances in vibration isolators using passive and hybrid dynamic vibration absorbers

Yu Du[a,*], Ricardo A. Burdisso[a], Efstratios Nikolaidis[b]

[a] *Vibration and Acoustics Laboratories, Mechanical Engineering Department, Virginia Tech., Blacksburg, VA 24060-0238, USA*

[b] *Mechanical, Industrial and Manufacturing Engineering Department, The University of Toledo, Toledo, OH 43606-3390, USA*

Received 24 February 2004; received in revised form 30 September 2004; accepted 16 October 2004
Available online 29 December 2004

Abstract

This paper discusses methods to improve isolator performance by controlling *Internal Resonances* (IRs), also referred as *wave effects*, in vibration isolators. The IRs are associated with the isolators' internal elastic motions that are due to the inertia existing in practical vibration isolators. It is well known that the IRs degrade the isolator performance as predicted by ideal massless isolator models. This degradation could be as high as 20–30 dB in the force transmissibility at the IR frequencies and 10–20 dB in the overall noise radiation from the foundation in the audible frequency range. This paper proposes two approaches of using dynamic vibration absorbers (DVAs) directly embedded into the isolator to attenuate the IRs. The first approach uses passive DVAs (PDVA). The effectiveness of this approach is investigated analytically using a 3 dof vibration model. It is shown that the PDVAs are very effective in attenuating the IRs and improve the isolator's performance at high frequencies. However, the PDVAs are less effective at low frequencies. To complement the effectiveness of the PDVA, an active control force is added, forming the hybrid DVA (HDVA) approach. The effectiveness of both the PDVA and the HDVA approaches, as well as the significance of the IRs in a commercial rubber mount, is also demonstrated experimentally. It is shown that an enhanced isolator with DVAs outperforms the original isolator without DVAs. Compared to the original isolator, in the isolation region of the experimental system, the PDVA approach reduces force

*Corresponding author. Current address: Adaptive Technologies, Inc., 2020 Kraft Drive, Suite 3040, Blacksburg, VA 24060, USA. Fax: +1 540 951 1993.
E-mail address: yudu@vt.edu (Y. Du).

0022-460X/$ - see front matter
doi:10.1016/j.jsv.2004.10.022

transmissibility by 18.5% and overall noise radiation by 4.3 dB. The HDVA approach reduces the force transmissibility and radiated noise by 92.2% and 9.1 dB, respectively.

1. Introduction

Current design methodologies for vibration isolation systems usually adopt the conventional massless isolator model, which predicts that the transmissibility of the isolator decreases at a rate of 12 dB per octave in the *isolation region* [1,2]. Here, the isolation range refers to the frequency region that is higher than the system resonant frequency, i.e. the region in which the transmissibility is less than one. For example, in a single degree-of-freedom (sdof) system the isolation region is defined as the frequency range above $\sqrt{2}f_0$, where f_0 is the system resonant frequency. The traditional isolator model considerably overestimates the performance of practical isolators, because it ignores the *internal resonances* (IRs) (also referred as *standing wave effects* in the literature), which are due to the distributed mass and elasticity of practical isolators [1–8]. The degradation effects of the IRs on vibration isolation have been noticed by many researchers since the 1950s. Kari indirectly pointed out the existence of the IR phenomenon by studying the dynamic stiffness of vibration isolators in the audible frequency range [3]. Harrison et al. [1], Snowdon [2], and Ungar [4] analytically showed that the force transmissibility of a practical isolator at the IR frequencies is 20–30 dB higher than that predicted by the traditional massless isolator model. In two recent publications, Du et al. [5,6] demonstrated that the adverse effects of the IRs are even more significant in multi dof systems and, in particular, from the perspective of noise radiation. They pointed out that significant improvement in the force transmissibility and a potential 10–20 dB reduction in the total sound power radiation in the high-frequency range could be obtained if the IRs were fully suppressed.

Although the importance of the IRs has been recognized, there is virtually no reported works on the control of such IRs to further improve the isolator performance. This is probably due to two main reasons. First, some previous researchers concluded that the IRs usually appear at high frequencies where the transmissibility level is either already very low or the performance at such high frequencies is no longer of practical concern [2]. Second, it was observed that the IRs can be damped by simply increasing the isolator's damping or applying another high damping material in parallel with the original isolator [7,8]. However, Du et al. [6] mentioned that it is not always practical to use high damping materials to attenuate the IRs because typically these materials exhibit poor returnability and greater drift, which greatly degrade the isolator's load capacity and the system's performance. Furthermore, because manufacturers continuously reduce the mass of equipments and increase their operating speed, it becomes increasingly important to achieve satisfactory isolation performance at high frequencies, especially when the noise is an important issue. Therefore, more effective ways for suppressing IRs in isolators should be investigated.

As mentioned earlier, to the best of the authors' knowledge, no approach for suppressing the IRs in vibration isolators has been reported in the open literature. However, some efforts that are relevant to the study presented herein have been found. Snowdon [9] discussed the feasibility of compound mounting systems consisting of isolators in which concentrated masses have been inserted. These masses are referred to as *intermediate masses* (IMs). Using compound mounts

results in lower transmissibility at high frequencies by increasing the mass of the isolators. However, this approach degrades the isolator performance at low frequencies. To alleviate this drawback, Snowdon [10] presented a method of using a dynamic vibration absorber (DVA) to suppress the secondary resonant peak (the first resonance frequency of an isolator). He demonstrated that the DVA approach could effectively attenuate the transmissibility at the secondary resonance of the compound system. Besides Snowdon, Neubert [11] investigated the effect of adding one or two DVAs to suppress the resonances of an axially excited bar. This work provides some valuable information for the suppression of the isolators' IRs in the sense that, for modeling purpose, the isolator is usually considered as a continuous rod, i.e. a bar, positioned between the primary system and the foundation [1,2,5,6].

The purpose of this paper is to investigate novel approaches to effectively suppress isolator resonances at the IR frequencies without significantly degrading the isolator performance at some other frequencies that are also of interest. To achieve this goal, this paper discusses the approach of using dynamic vibration absorbers (DVAs) directly embedded into the isolator to attenuate the IRs. First, it is proposed to use passive DVAs (PDVA). In contrast to Snowdon's work [10], where one PDVA was attached to a concentrated mass, in this study, multi-PDVAs are attached to the isolator. It is found that the PDVA-enhanced isolator effectively suppress the IRs that usually occur at high frequencies (e.g. >500–1000 Hz). On the other hand, adding PDVAs degrades the isolator performance at low frequencies (e.g. <500–1000 Hz). This adverse effect is due to the newly introduced resonances corresponding to the dynamics of the PDVAs. One way to further improve the effectiveness of vibration absorbers, particularly at low frequencies, is the addition of an active component. The second approach proposed in this paper is to use a passive/active or hybrid DVA (HDVA)-enhanced isolator to attenuate the IRs, thus improving the broadband performance of vibration isolators. In the following sections, the feasibility and effectiveness of PDVA- and HDVA-enhanced isolators will be presented both analytically and experimentally.

2. Theory

2.1. Concept of using DVAs to suppress the IRs

Dynamic vibration absorbers are essentially mass–spring–damper subsystems which, when connected to a main vibrating system, are capable of absorbing the vibration energy at the attachment point of the main system. It is common practice to use a DVA to attenuate the resonances in a vibration system. To illustrate the concept of using DVAs to control the IRs, Fig. 1 shows the force transmissibility of a sdof system as a function of the driving frequency. The sdof vibration system is illustrated in Fig. 2 in which a rigid primary mass, m, is connected to a rigid foundation through a realistic isolator (i.e. the isolator is considered as a continuous system with distributed mass and thus it has IRs) and is excited by an external force, F_0. The mathematical models for generating the force transmissibility of a sdof system with a realistic isolator and a DVA-enhanced isolator can be found in Ref. [6] and Section 2.3 of this paper, respectively. The dotted line in Fig. 1 is for the isolator without a DVA. As expected, there are two IRs above 1000 Hz. For comparison, the solid line represents the case of the enhanced isolator with one DVA attached to the middle cross-section of the isolator and tuned to the first IR

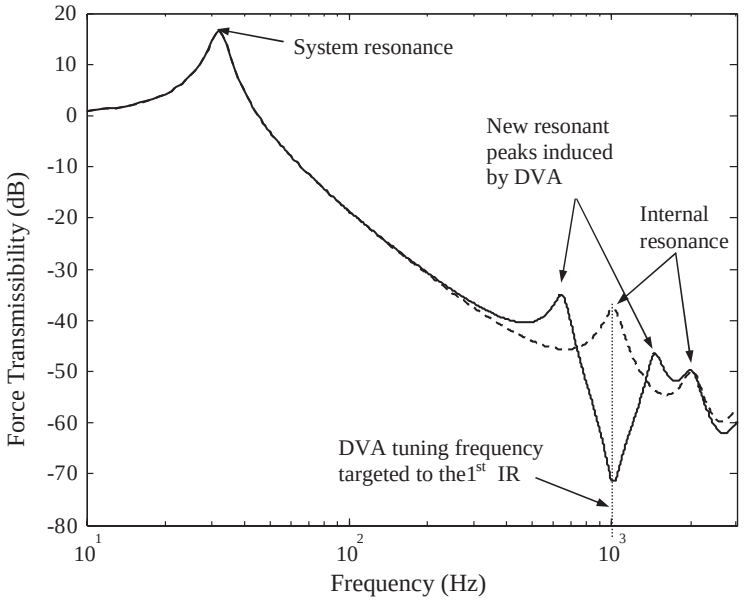

Fig. 1. Concept of using DVAs to suppress the IRs: - - - - , without DVA; ——, with DVA.

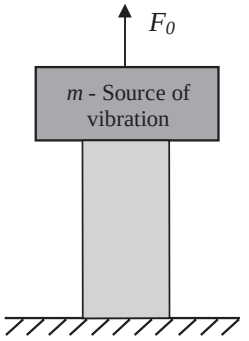

Fig. 2. A sdof vibration system consisting of a rigid primary mass m connected to a rigid foundation through an isolator. The primary mass is excited by an external force F_0.

frequency of the isolator. As a result of adding a DVA, the amplitude of the force transmissibility at this frequency is greatly reduced. On the other hand, two new resonant peaks appear at each side of the original IR peak due to the DVA dynamics, i.e. splitting of the resonance due to the DVA. However, the amplitudes of the new resonances are much lower than those of the original IR peak when the DVA parameters are properly selected. Therefore, the DVA-enhanced isolator allows less force, i.e. energy, to be transmitted to the foundation. This observation is the basis of using DVAs to suppress the IRs, and to improve the isolator performance.

Although the concept of using DVAs to suppress the isolator's IRs introduced above is similar to that of using DVAs to suppress the system resonances of a vibrating mass, their implementations are different [12]. When designing a DVA for suppressing a specific system

resonance, for example the system resonance indicated in Fig. 1, the DVA is always tuned to this frequency and attached to the primary mass m (refer to Fig. 2). However, when designing DVAs for suppressing the IRs of a continuous vibrating system, i.e. the isolator, there are more practical issues, in addition to determining the DVA parameters that need to be resolved. These issues are the determination of the number and the location of the DVAs, and the selection of the physical connection method between the DVAs and the isolator. These three issues are discussed next from both theoretical and practical perspectives.

2.1.1. Number of DVAs

Since one DVA normally can only attenuate one resonance, the number of DVAs that are to be used depends on the number of resonances that are to be suppressed. The problem of determining the number of the IRs that are needed to be controlled is two-fold in nature. First, it is required to determine the frequency range in which the isolator performance is of the greatest interest for a practical vibration isolation problem. Second, it is important to determine the most significant IRs in this frequency range. These most significant IRs greatly degrade the isolator performance; thus they need to be attenuated to improve the performance.

The excitation input of practical isolation systems could be either harmonic, such as the excitation due to an unbalanced mass of rotational machinery (e.g. engines), or broadband, such as the road surface excitation applied to vehicles. For either case, there is an upper limit in the frequency range of interest. For example, the highest disturbance frequency due to the engine depends on the rotation speed of the crankshaft while the highest excitation frequency due to the road surface is limited by the speed of vehicles and the roughness of road surfaces. The normal frequency range, in which the practical excitation energy is significant for mechanical vibrations, is from several tens to several thousands Hz. Consequently, the isolator performance in this frequency range is of the primary concern. In most practical situations, only a handful of IRs of an isolator lie within this frequency range.

On the other hand, it has been shown by many researchers that the amplitudes of the higher order IRs decrease rapidly with the frequency [1-2,4–9], i.e. the higher order IRs are effectively damped out by the isolator material damping. It should be pointed out that these results were predicted under the assumption that the isolator can be modeled as a ''long-rod'', i.e. the lateral deformation of the isolator under the longitudinal excitation is ignored. A more complex model based on the theory developed by Love [13] that accounts for the ''lateral-inertia'' shows that the magnitude of the higher order IRs decreases even more rapidly than what was predicted earlier [1–9]. That is, the first several IRs have the most practical significance in terms of the isolator performance. In this paper, without loss of generality, the first two IRs of the isolator are chosen to be controlled and accordingly two DVAs are used.

2.1.2. DVA attaching positions

Since the DVA functions by absorbing the vibratory energy, it is always desirable to attach the DVA at the location of maximum vibration in the isolator. The best attaching position for DVAs is then determined by examining the deformation of the isolator at the IRs, i.e. by examining the isolator modes. To this end, the displacement fields of an isolator in a sdof system at the first few resonant frequencies are calculated and are plotted in Fig. 3. Note that the first resonance in this figure corresponds to the system resonance. It is observed that at the system resonance, the top of

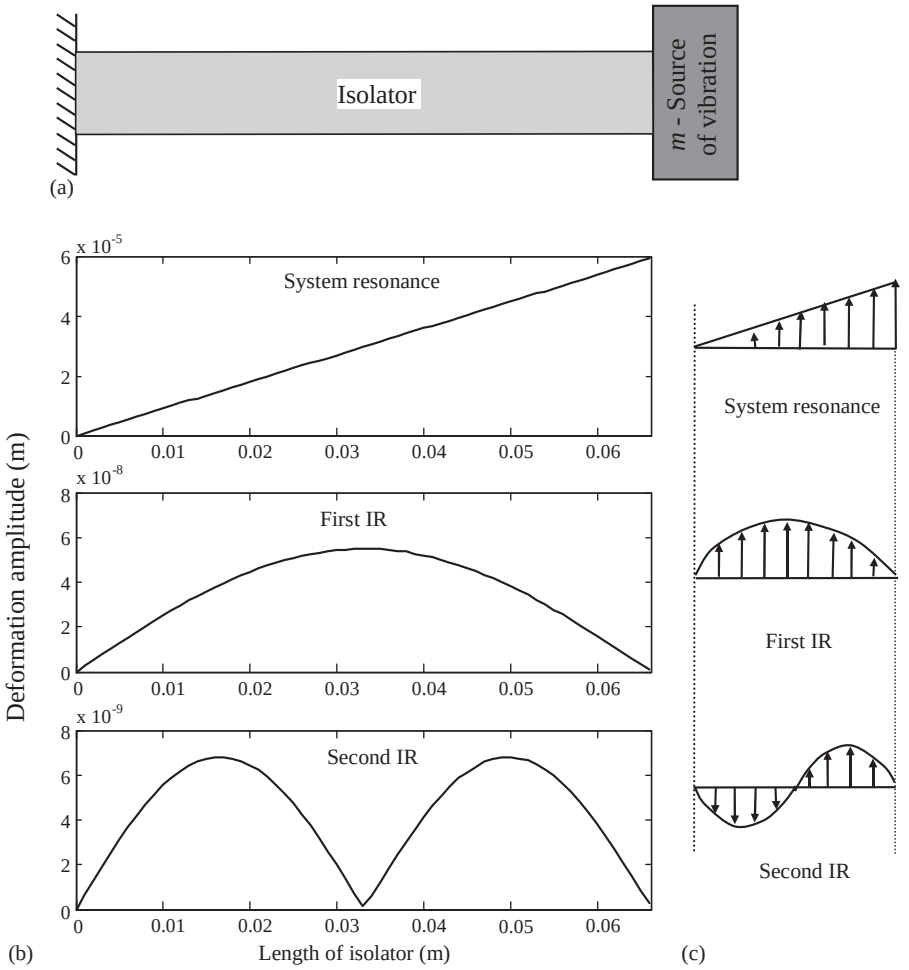

Fig. 3. (a) Schematic of a sdof isolator system, (b) isolator deformation and (c) mode shapes at the system resonance and the first two IR frequencies.

the isolator has the largest displacement, which is equal to the motion of the primary mass. In this case, the DVA is attached to the primary structure when the system resonance is to be attenuated. However, this configuration is not desirable for suppressing the IRs because the ends of the isolator are virtually motionless at the IRs. Indeed, Fig. 3(b) shows that in terms of the IRs, the mode shapes of the isolator in the vibration system shown in Fig. 3(a) can be approximated by the mode shapes of the isolator when it undergoes longitudinal vibration with pinned–pinned boundary condition. The maximum displacement at IR modes takes place within the isolator, which indicates that the DVA should be attached or embedded directly into the isolator to suppress IRs. This conclusion is further validated from the results in Fig. 4.

Fig. 4 shows the force transmissibility through the isolator in Fig. 3(a). To suppress the first IR, a DVA is integrated into the isolator and is tuned to the first IR frequency. Three attaching positions are considered at distances equal to $\frac{1}{8}$, $\frac{1}{4}$, and $\frac{1}{2}$ of the total length of the isolator measured

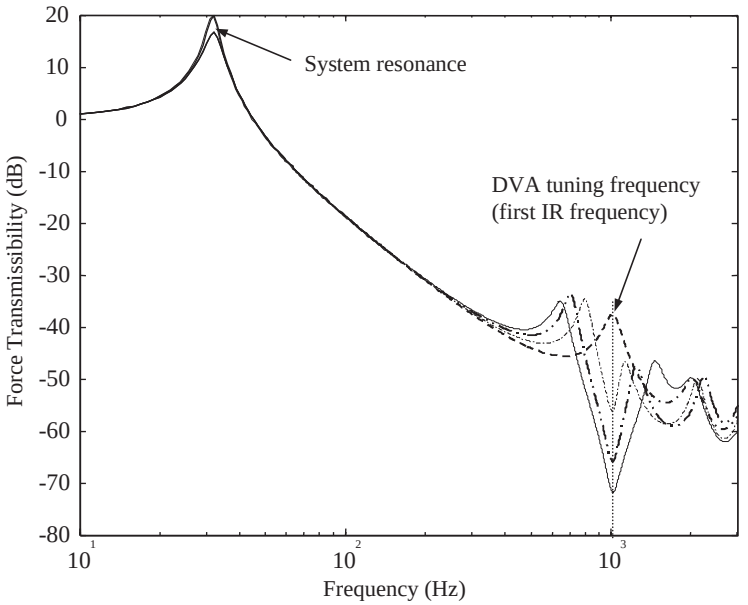

Fig. 4. Illustration of the best DVA attaching position for suppressing the first IR in a sdof system with rigid foundation: no DVA (- - - -); a DVA is attached at a locations with distance $\frac{1}{8}$ (- · · · · · · -), $\frac{1}{4}$ (— · · —); and $\frac{1}{2}$ of the length from the top of the isolator (——).

from its top. In these three cases, the DVA parameters (stiffness, damping and tuning frequency) are the same. For comparison, the curve for the case of an isolator without DVA is also plotted in the same figure. It is observed that when the DVA is placed at the center of the isolator, the amplitude of the transmissibility curve at the first IR frequency is reduced more than when it is placed elsewhere. As expected, this result implies that the center of the isolator is the best position to attach a DVA to suppress the first IR, i.e. the anti-node of that mode. Referring to Fig. 3(b), the maximum deformation of the isolator appears at the center cross-section of the isolator at the first IR mode. Likewise, the ''one-quarter'' position from both ends of the isolator is the best place for the DVA to suppress the second IR because the maximum displacement appears at that position at the second IR mode (Fig. 3).

As mentioned earlier, this study uses two DVAs to suppress the first two IRs. Based on the analysis in the previous paragraph, and the fact that the two DVA cannot be too close to each other in practice, the two DVAs are placed at the positions with distances of one-quarter length from both ends of the isolator. This configuration is optimal for suppressing the second IR and is also acceptable for controlling the first IR.

2.1.3. Intermediate mass

When a DVA is to be directly embedded into a viscoelastic isolator the DVA needs to be connected to a support attached to the isolator. This support could be a ring or a thin plate inside the isolator body. The stiffness of this support is normally very high compared to the stiffness of the isolator so that its influence on the isolator stiffness is negligible. On the contrary, the mass of this support may be too large to be neglected when compared to the mass of the isolator and the

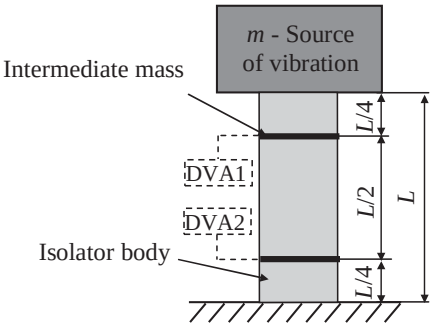

Fig. 5. Schematic of the application of the intermediate masses.

DVA. When the mass of the support cannot be ignored, it acts as a concentrated mass in the isolator body and separates the isolator into two segments. This mass is called *intermediate mass* (IM). An isolator with IMs is referred as *compound isolator* [9]. Fig. 5 shows such a compound isolator that incorporates two concentrated masses for attaching two DVAs (denoted in dotted lines).

The IMs affect the isolator's dynamics in both a desirable and undesirable ways and it is important to understand their behavior. Consider the sdof system with the compound isolator shown in Fig. 5 (without DVAs), whose force transmissibility is plotted as the solid line in Fig. 6. For comparison, the transmissibility for the system without IMs is also shown by the dotted line. It is seen that above 1100 Hz, the transmissibility of the compound system decreases at a much higher rate by inserting the IMs. That is, the amplitudes of the IRs above 1100 Hz are greatly reduced, which is the advantage of incorporating the IMs. This phenomenon is consistent with the results for the massless compound isolator presented in literature [9,10]. However, the first two IRs are shifted towards lower frequencies due to the addition of IMs, which considerably impairs the isolator performance in the middle frequency range. This adverse effect of adding IMs is shown in later sections to be effectively controlled by incorporating the DVAs. Thus, the IMs and the DVAs work together to effectively control the isolator's IRs.

2.2. Using hybrid DVA to suppress the IRs

It has been shown that it is feasible to attach two passive DVAs to an isolator at the "one-quarter-length" position to attenuate the IRs. However, it is also known that the PDVAs are only effective in a narrow effective frequency band. Because a PDVA works best at its tuning frequency, it may become ineffective when the resonant frequencies of the primary structure and/or the disturbance spectrum may change. In HDVA approach an active element is used together with passive DVA elements to further improve the isolator performance. Based on the previously proposed PDVA-enhanced isolator configuration, a HDVA-enhanced isolator can be constructed by adding an active force component(s). There are several options for the incorporation of the active component(s) in the PDVA-enhanced isolator. In a classical implementation, the active component in the form of a control force pair is applied between the absorber's mass and the primary structure in parallel to the elastic (i.e. passive) element used to mount the absorber

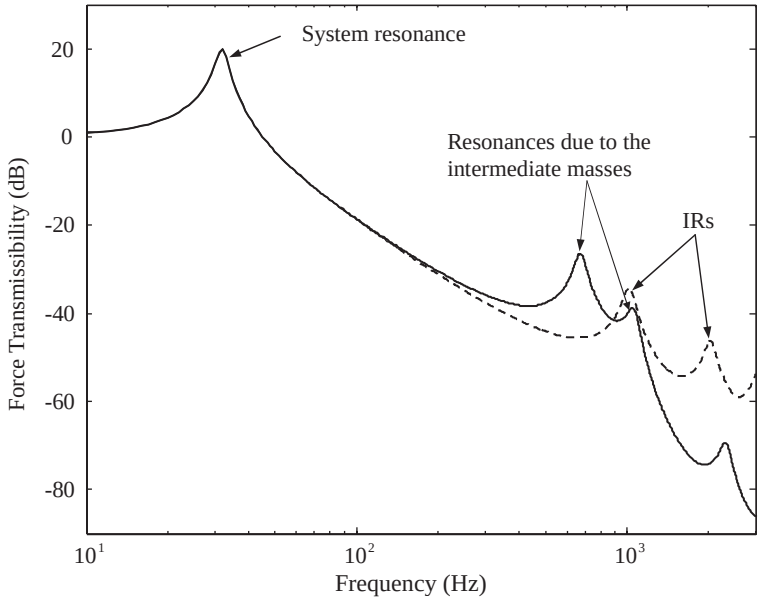

Fig. 6. Comparison of the force transmissibility of compound and simple system with realistic isolator: - - - -, simple system (no IMs); ———, compound system (with IMs).

[14,15]. This configuration is illustrated in Fig. 7(a). Its main drawback is that it leads to the need of adding two active components or actuators, i.e. one for each DVA, with the consequent increase in system complexity. A second potential configuration that can use a single actuator is shown in Fig. 7(b). In this configuration, the two DVAs are connected to the same location in the isolator with the active element acting between the DVAs masses. Indeed, this implementation has been recently proposed and demonstrated experimentally to be very effective [15]. This configuration is called dual reaction masses HDVA or simply *dual-mass* HDVA that requires a single control element. Burdisso and Heilmann [15] compared the performance of the conventional single-mass and the dual-mass HDVA in detail. They concluded that the dual-mass HDVA only needs half of the control energy required by the single-mass HDVA to reduce the response of the primary structure by the same amount. The disadvantage of implementing this dual-mass HDVA to control the IRs is that in the passive configuration it was determined that mounting the two DVA masses at the two "one-quarter-length" locations is preferred from a practical point of view. Thus, the configuration shown in Fig. 7(c) is proposed in this work. In this approach, the active force is also applied between the two DVA masses and thus it takes advantage of the demonstrated benefits of the dual-mass HDVA. In contrast to the second configuration, the two DVAs in Fig. 7(c) are, however, connected to the isolator body at different positions, i.e. each is $\frac{1}{4}$ of the isolator's total length away from the nearest end of the isolator.

2.3. Model of the PDVA- and HDVA-enhanced isolators

Fig. 8 illustrates the proposed configuration of a DVA-enhanced isolator, which consists of a cylindrical isolator made of rubberlike material with two embedded DVAs. The DVAs are placed

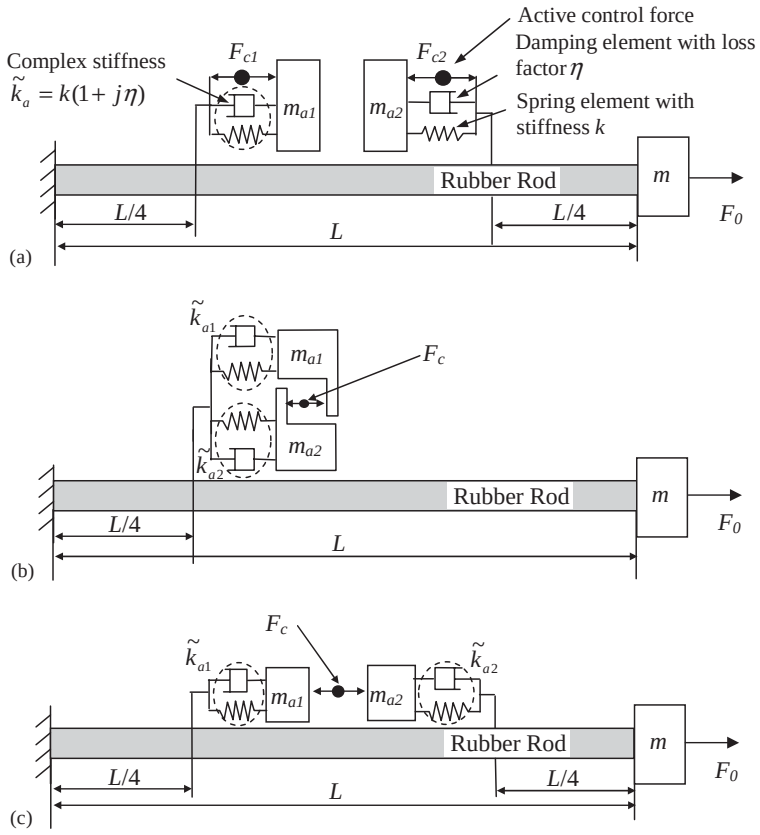

Fig. 7. Schematic of potential control configurations: (a) two single-mass HDVA, (b) dual-mass HDVA and (c) two DVAs connected to the primary structure at different positions with an active force acting in between the two DVA masses. The foundation structure is assumed to be rigid.

in the cylindrical cavity inside the isolator and each of them is connected to the isolator at the "one-quarter-length" position through a thin plate (i.e. the IM). The isolator has density ρ, length L and complex modulus $\tilde{E} = E(1 + j\eta)$, where E is the Young's modulus and η is the loss factor of the isolator. Each DVA has mass m_{ai} and complex stiffness $\tilde{k}_{ai} = k_{ai}(1 + j\eta_{ai})$, where k_{ai} is the spring constant and η_{ai} is the loss factor of the DVA spring ($i = 1, 2$). The upper and lower IMs are denoted as m_{iu} and m_{il}, respectively. The isolator is separated by the two IMs into three segments marked as ①, ② and ③ from top to bottom. Therefore, this DVA-enhanced isolator can be considered as a combination of three-component isolators (isolators ①, ② and ③), two thin plates (IMs), and two DVAs. An active force, F_c, is applied between the two DVA masses to model a HDVA-enhanced isolator. Notice that no damping or spring element couples the two DVA masses, in parallel with the active force. When the active force F_c is zero, this HDVA-enhanced isolator is simplified to a PDVA-enhanced isolator. Therefore, the HDVA- and PDVA-enhanced isolators can be represented using a single mathematical model with an active force, which is zero for the latter isolator.

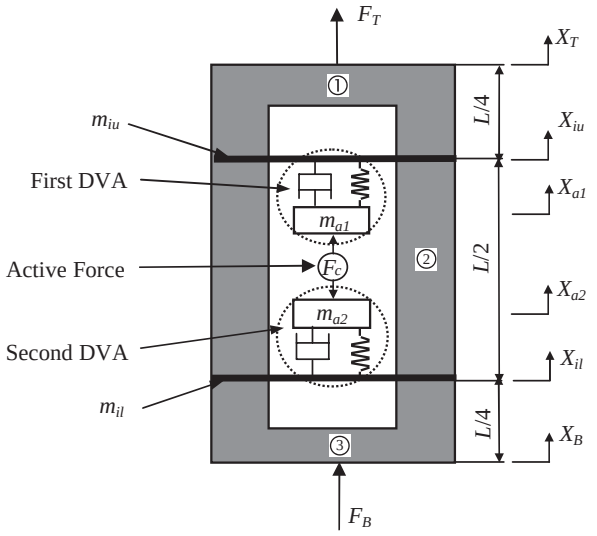

Fig. 8. Configuration of the PDVA ($F_c = 0$) and HDVA ($F_c \neq 0$) enhanced isolators.

The development of the dynamic model of this DVA-enhanced isolator involves finding the relationship between the two external forces (F_T and F_B) and the resulting displacements (X_T and X_B) at the two ends of the isolator. The equations of motion (EOMs) of the DVA-enhanced isolator are written by coupling the dynamics of the three-component isolators, the IMs and the DVAs. That is

$$(-\omega^2[M] + [K_s]) \begin{Bmatrix} X_T \\ X_{iu} \\ X_{a1} \\ X_{a2} \\ X_{il} \\ X_B \end{Bmatrix} = [D_{\mathrm{DVA}}] \begin{Bmatrix} X_T \\ X_{iu} \\ X_{a1} \\ X_{a2} \\ X_{il} \\ X_B \end{Bmatrix} = \begin{Bmatrix} F_T \\ 0 \\ F_c \\ -F_c \\ 0 \\ F_B \end{Bmatrix}, \tag{1}$$

where X_{iu}, X_{il}, X_{a1} and X_{a2} represent the displacements of the upper IM, the lower IM, the first DVA and the second DVA, respectively. The mass matrix $[M]$ is given by

$$[M] = \begin{bmatrix} 0 & & & & & \\ & m_{iu} & & & & \\ & & m_{a1} & & & \\ & & & m_{a2} & & \\ & & & & m_{il} & \\ & & & & & 0 \end{bmatrix}, \tag{2}$$

and the stiffness matrix $[K_s]$ is given by

$$[K_s] = \begin{bmatrix} D_1^d & -D_1^o & 0 & 0 & 0 & 0 \\ -D_1^o & D_1^d + D_2^d + \tilde{k}_{a1} & -\tilde{k}_{a1} & 0 & -D_2^o & 0 \\ 0 & -\tilde{k}_{a1} & \tilde{k}_{a1} & 0 & 0 & 0 \\ 0 & 0 & 0 & \tilde{k}_{a2} & -\tilde{k}_{a2} & 0 \\ 0 & -D_2^o & 0 & -\tilde{k}_{a2} & D_2^d + D_3^d + \tilde{k}_{a2} & -D_3^o \\ 0 & 0 & 0 & 0 & -D_3^o & D_3^d \end{bmatrix}, \tag{3}$$

where D_i^d and D_i^o, for $i = 1, 2, 3$, are the terms of the dynamic stiffness matrix of the three components of the isolator, ①, ② and ③. These terms are calculated from the isolator material properties [6,12]. Note that the inertia of the isolator is included in the terms D_i^d and D_i^o.

Replacing Eqs. (2) and (3) into Eq. (1) yields the dynamic stiffness matrix, i.e. the dynamic model, of the DVA-enhanced isolator:

$$[D_{\mathrm{DVA}}] = \begin{bmatrix} D_1^d & -D_1^o & 0 & 0 & 0 & 0 \\ -D_1^o & T_{22} & -\tilde{k}_{a1} & 0 & -D_2^o & 0 \\ 0 & -\tilde{k}_{a1} & T_{33} & 0 & 0 & 0 \\ 0 & 0 & 0 & T_{44} & -\tilde{k}_{a2} & 0 \\ 0 & -D_2^o & 0 & -\tilde{k}_{a2} & T_{55} & -D_3^o \\ 0 & 0 & 0 & 0 & -D_3^o & D_3^d \end{bmatrix}, \tag{4}$$

where $T_{22} = -\omega^2 m_{iu} + D_1^d + D_2^d + \tilde{k}_{a1}$, $T_{33} = -\omega^2 m_{a1} + \tilde{k}_{a1}$, $T_{44} = -\omega^2 m_{a2} + \tilde{k}_{a2}$ and $T_{55} = -\omega^2 m_{il} + D_2^d + D_3^d + \tilde{k}_{a2}$.

2.4. Model of the isolation system with PDVA- and HDVA-enhanced isolators

To investigate the effectiveness of the proposed PDVA and HDVA approaches, the PDVA- and HDVA-enhanced isolators are modeled into an isolation system. Since a 3 dof vibration model better represents a practical vibration system more accurately than the traditionally used sdof model [5-6,12], this model is used to assess the performance of the PDVA-enhanced isolator. However, for simplicity and clarity, a sdof model is employed when evaluating the characteristics of the required active control force in the HDVA-enhanced isolator. The isolator performance is evaluated by calculating the force transmissibility through the isolator and the radiated acoustic power of the foundation.

2.4.1. A 3 dof vibration isolation model incorporating the PDVA-enhanced isolator

Fig. 9(a) shows a schematic of the 3 dof model that consists of a rigid primary mass connected to a flexible foundation through three isolators. For clarity, this analytical model is referred to as the *reference system* in this paper. All joints between the isolators and the primary mass, and between the isolators and the foundation are pinned. Therefore, each isolator transfers force along its axis only. The three dofs of the primary mass are characterized by the three vertical

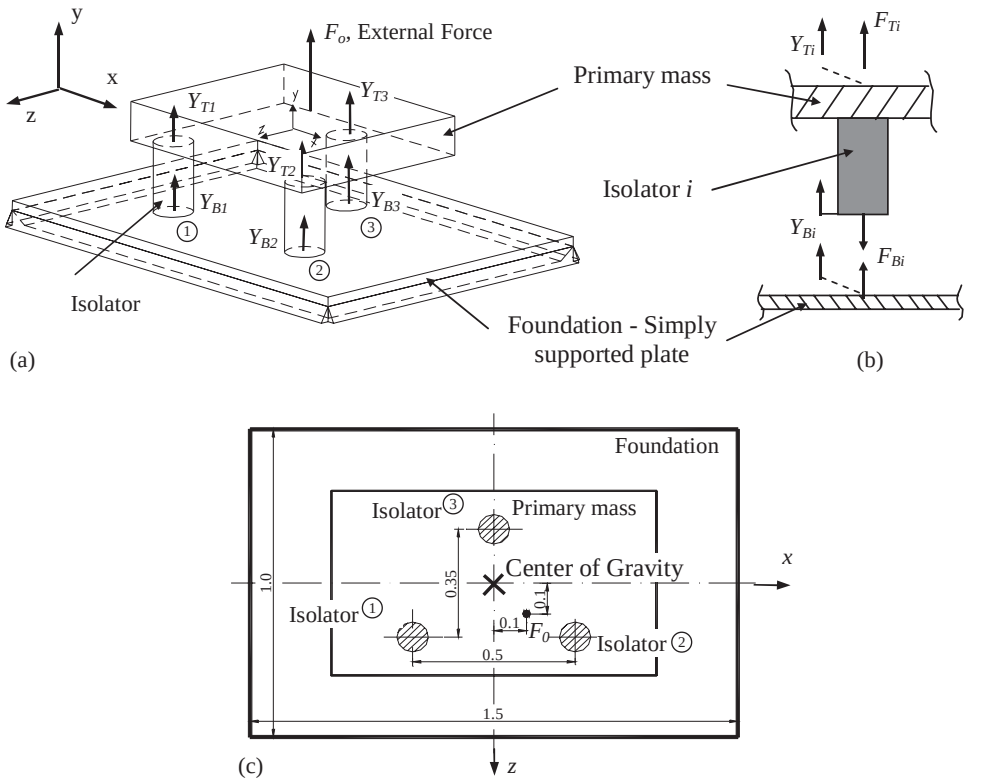

Fig. 9. Schematic plot for (a) the 3 dof model and (b) the free body diagram when separating the foundation from the primary mass isolators substructure at the ith isolator and (c) illustration for the layout of the isolation system.

translations, denoted as Y_{Ti} $(i = 1, 2, 3)$, at the mounting points between the isolators and the primary mass. Correspondingly, the translational displacements at the interface between the isolators and the foundation are denoted as Y_{Bi}. The foundation is modeled as a simply supported rectangular plate that radiates noise under the excitation of the forces transmitted through the three isolators. The external disturbance to the system is a concentrated force with amplitude F_0 acting at an arbitrary location on the primary mass.

Fig. 9(b) illustrates the free body diagram when the foundation is separated from the primary mass-isolators substructure at the ith isolator, where i can be 1, 2 and 3. Notice in this figure, the external disturbance F_0 is split into three components denoted as F_{Ti}. These three components are statically equivalent to F_0 and act at each dof of the primary mass [6,12]. As a result of the external disturbance, a transmitted force, F_{Bi}, is present at the bottom of each isolator. The amplitude of the transmitted force depends on the properties of the isolator. The EOMs of the coupled 3 dof system are derived by first modeling the substructures consisting of (a) the primary mass and isolators, and (b) the foundation separately. The two substructures are then coupled by imposing conditions for continuity of forces and displacements at their interfaces, i.e. at the isolators' attachment to the foundation [6]. The geometrical positions of the external force, the primary mass, the three isolators, and the foundation are illustrated in Fig. 9(c).

The system parameters are selected on the basis of information about practical vibration systems. For example, the primary mass used in the simulation is 27.8 kg and the moments of inertia about its x-axis and the z-axis are 0.44 and 0.82 kg/m^2, respectively. To induce rotations, the external force F_0 is applied off the center of gravity of the primary mass at $(x_F, z_F) = (0.1, 0.1)$. This excitation force is assumed to have constant amplitude in the frequency range from 1 to 3000 Hz. The three isolators are identical with length 0.066 m and cross-sectional area 0.00123 m^2. The isolators are made of viscoelastic material with density 1103 kg/m^3, Young's modulus 20 MPa, and loss factor 10%. The selection of these isolator parameters was based on both the properties of a commercial rubber mount manufactured by Lord Corporation and the values presented in Refs. [1,16]. The foundation is a $1.5 \times 1 \times 0.02$ m rectangular steel plate with modulus of elasticity 2×10^5 MPa, density 7800 kg/m^3, loss factor 1%, and Poisson's ratio 0.28. This foundation may simulate a typical flexible base, such as the body of a car. According to the above parameters, the three system resonances for this 3 dof model appear at 31.2, 41.8 and 52.4 Hz while the first two IRs occur at much higher frequencies of 1017 and 2033 Hz.

As mentioned earlier, the isolator performance is evaluated by calculating the force transmissibility of each isolator and the radiated acoustic power of the foundation. After obtaining the system's EOMs, the transmitted force through each isolator is calculated. The force transmissibility through each isolator, T_i, is then defined as the magnitude of the transmitted force when the amplitudes of all the input force components, F_{Ti}, are all equal to one [6]. That is,

$$T_i = |F_{Bi}| \quad \text{when} \quad |F_{T1}| = |F_{T2}| = |F_{T3}| = 1. \tag{5}$$

Using the wavenumber transform, the radiated sound power, P, for a plate structure embedded in a baffle is given as [17]

$$P = \frac{\omega \rho_a}{8\pi^2} \iint\limits_{k \geqslant \sqrt{k_x^2 + k_z^2}} \frac{|V(k_x, k_z)|^2}{\sqrt{k^2 - k_x^2 - k_z^2}} \, \mathrm{d}k_x \, \mathrm{d}k_z, \tag{6}$$

where ρ_a is the density of the air, k_x and k_z are variables of integration, $k = \omega/c$ is the acoustic wavenumber, ω is the frequency of the external excitation, c is the speed of sound in air, and $V(k_x, k_z)$ is the 2D velocity wavenumber transform of the plate response. To comply with the radiation condition, the integration in Eq. (6) is over the supersonic wave region, i.e. $k \geqslant \sqrt{k_x^2 + k_z^2}$.

Eqs. (5) and (6) assess the isolator performance at different frequencies in terms of the vibration transmissibility and the noise radiation, respectively. Since the primary concern in the vibration isolation design is the isolator performance in a specific frequency range, the root-mean-squared (rms) value of the transmissibility and the total acoustic power in this range are used as the metrics for performance comparison. Since the highest system resonance for the reference system is at 52.4 Hz and the highest disturbance frequency is 3000 Hz, the 200–3000 and 500–3000 Hz frequency bands are considered for evaluating performance. The former frequency range is the isolation region of this reference system, while the latter range excludes the effect of the system resonances and thus it emphasizes the isolator performance in the IR frequency region.

2.4.2. A sdof vibration isolation model incorporating the HDVA-enhanced isolator

The 3 dof model described above can be easily simplified into a sdof model by combining the three isolators into one equivalent isolator and allowing the primary mass, m, to move only in the vertical direction under the excitation of the external force F_0. Allowing a non-zero active force and using the same nomenclature as presented in Eq. (1), the sdof vibration model incorporating the HDVA-enhanced isolator can be written as

$$\left(-\omega^2\begin{bmatrix} m & & & & & \\ & 0 & & & & \\ & & 0 & & & \\ & & & 0 & & \\ & & & & 0 & \\ & & & & & 0 \end{bmatrix} + [D_{\mathrm{DVA}}]\right)\begin{Bmatrix} X_T \\ X_{iu} \\ X_{a1} \\ X_{a2} \\ X_{il} \\ X_B \end{Bmatrix} = \begin{Bmatrix} F_0 \\ 0 \\ F_c \\ -F_c \\ 0 \\ F_B \end{Bmatrix}. \tag{7}$$

3. Numerical simulation

3.1. PDVA-enhanced isolator performance

In order to achieve good attenuation results, it is critical to carefully select the DVA parameters. Du et al. [12] performed a parametric study on the effects of the DVA parameters on the isolator performance. This study provides insight into the effect of each design variable (DVA mass, loss factor, tuning frequency and the IM) on the isolator performance. As a conclusion from this parametric study, it was suggested that the DVA parameters should be optimally designed to most effectively suppress the IRs and achieve the best isolator performance in a certain frequency range of concern. That is, the optimum values of the DVA parameters can be obtained by minimizing an objective function expressing the isolator performance, such as the force transmissibility or the radiated acoustic power.

In this section, the DVA parameters in the model of the PDVA-enhanced isolator are optimized by minimizing the force transmissibility through the isolators shown in Fig. 9. For simplicity, the parameters of the three PDVA-enhanced isolators are assumed to be identical and the IM is kept constant at 0.05 kg in the optimization process. To yield practically feasible values, lower and upper bounds are given to each design variable in the optimization routine. The practical range for the DVA mass is assumed to be 0–0.15 kg. The loss factor is bounded between 0% and 40%, because larger damping is difficult to achieve in practice. The range for the tuning frequency is 350–1200 Hz. A detailed description of the parameter optimization is beyond the scope of this paper and can be found in Ref. [18]. The optimization was performed for the two frequency ranges that were mentioned previously, i.e. 200–3000 and 500–3000 Hz. Table 1 lists the optimized DVA parameters. It is clear that the optimum DVA parameters are sensitive to the frequency range of interest.

In the following two subsections, the performance of the *original isolator* (i.e. no DVA is attached) and the PDVA-enhanced isolator are compared based on the reference system described in Fig. 9. This comparison shows the theoretical improvements that can be achieved by using DVAs to suppress the IRs. The performance of the DVA-enhanced isolator, as compared to the

Table 1
DVA parameters optimized for the force transmissibility

		Target frequency range for the optimization (Hz)	
		200–3000	500–3000
Mass (kg)	DVA 1	0.097	0.15
	DVA 2	0.06	0.15
Loss factor	DVA 1	40%	7%
	DVA 2	40%	40%
Tuning frequency (Hz)	DVA 1	350	553
	DVA 2	628	1032

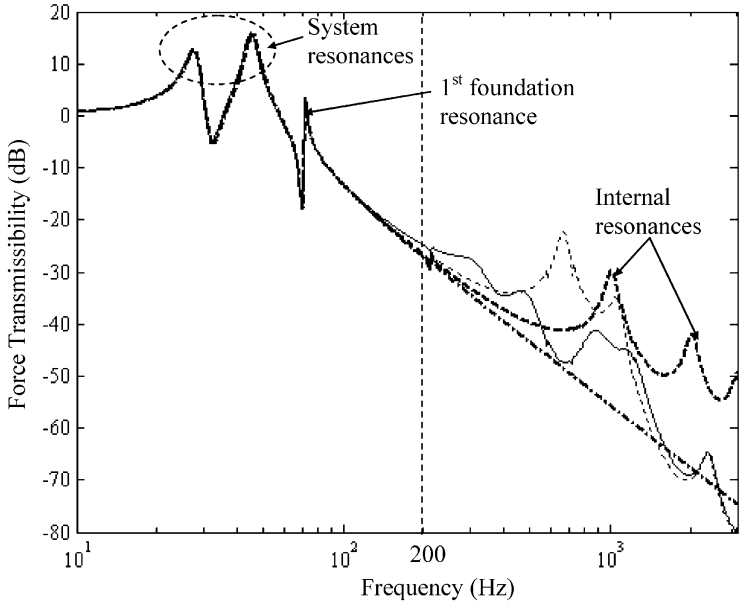

Fig. 10. Force transmissibility of isolator 1 in the reference system when the PDVA parameters are optimized for the force transmissibility within (200–3000 Hz): ———, PDVA-enhanced isolator; — · —, ideal massless isolator; - - - ·, original isolator, - - - -, compound isolator with two IMs.

original isolator, is evaluated in terms of the force transmissibility of isolator 1 and the radiated acoustic power of the foundation.

The transmissibility for the PDVA-enhanced isolator 1 (solid line) optimized by minimizing the transmitted forces in the 200–3000 Hz range is plotted in Fig. 10. For comparison, the transmissibility curves for the system with the original (dashed line) isolator, the ideal massless (dash–dotted line) isolator and the compound isolator (dotted line) that only has the IMs are also shown in the same figure. It is seen that, as expected, the IRs of the original isolator are largely attenuated by the PDVA approach. Moreover, the transmissibility amplitude beyond 2000 Hz of the PDVA-enhanced isolator is almost as low as that of the ideal massless isolator. Since the PDVAs introduce new resonances at low frequencies, it is observed that the transmissibility of the

enhanced isolator between 200 and 500 Hz is slightly higher than that of the practical isolator. However, in general, the decreasing rate of the transmissibility curve above 200 Hz for the PDVA-enhanced isolator is much higher than that for the original isolator and tends to approach the behavior of the massless one. In addition, it is interesting to notice that the compound isolator has a high-frequency performance that is as good as the PDVA-enhanced isolator. This good performance is due to the addition of the IMs, i.e. the "blocking masses" as suggested in Ref. [9]. However, in contrast to the good performance of the PDVA-enhanced isolator in the mid frequency range, the IMs in the compound isolator also introduce significant resonances such as the resonances around 650 and 1050 Hz in Fig. 10. Since the difference between the PDVA-enhanced isolator and the compound isolator is the presence of the PDVAs, it can be concluded that the resonances due to the IMs are effectively attenuated by the PDVAs.

Fig. 11 compares the transmissibility of the enhanced isolator with PDVA parameters optimized for the transmissibility within 500–3000 Hz. It is observed that the PDVA approach results in considerable reductions in the force transmissibility. In the frequency band of interest, the transmissibility of the enhanced isolator is 10–30 dB lower than that of the original isolator. At some frequencies (e.g. 500–1000 Hz), the enhanced isolator performs even better than the massless isolator. However, the transmissibility of the enhanced isolator around 350 Hz is significantly higher than that of the original isolator.

A comparison between DVA parameters used in Figs. 10 and 11 (refer to Table 1) provide additional physical insight. It is seen that both DVA masses took the maximum value (upper constrain bound) of 0.15 kg for the 500–3000 Hz range case. This is because the larger DVA mass helps reduce the transmissibility at high frequencies by shifting the IRs towards lower frequencies

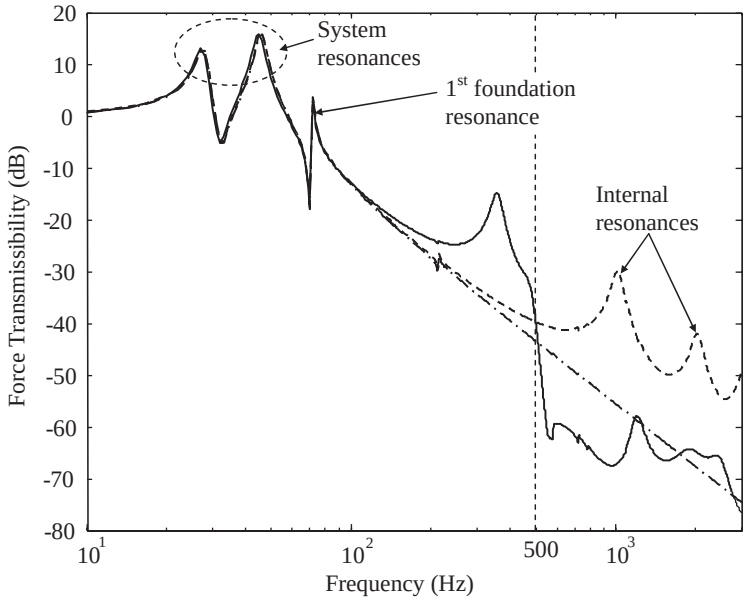

Fig. 11. Force transmissibility of isolator 1 in the reference system when the PDVA parameters are optimized for the force transmissibility within (500–3000 Hz): ———, DVA-enhanced isolator; — · —, ideal massless isolator; - - - -, original isolator.

[12]. On the other hand, the DVA masses for the case where the frequency range is 200–3000 Hz are relatively small so as to keep the response at the resonances as small as possible. Moreover, both high damping and low tuning frequencies were chosen for this case. This result shows the effort by the optimizer to attenuate the low-frequency resonances. In fact, the optimizer always tries to select the best parameters to maximize the effectiveness of the DVAs over a wide range of frequencies. The effectiveness of the optimized DVAs at low and mid frequencies and the advantage of the high decreasing rate of the transmissibility at high frequencies introduced by the IM ensure a broadband performance improvement of the PDVA approach.

To evaluate the broadband performance, Table 2 lists the RMS transmissibility for the results in Figs. 10 and 11. It is seen that the RMS transmissibility of the PDVA-enhanced isolator in the 500–3000 Hz range is only one-tenth of that of the practical isolator and is even smaller than the RMS value of the ideal massless isolator. This comparison shows the effectiveness of using PDVAs to suppress the IRs at high frequencies. In contrast, it is also observed that the RMS transmissibility for the enhanced isolator optimized in the frequency range from 200 to 3000 Hz is slightly greater than that of the original isolator, which suggests that PDVAs could be ineffective when the performance in a broad frequency range is important. This result is easily explained since in Fig. 10, it is clear that significant reduction in transmissibility achieved above 500 Hz by the addition of PDVAs is offset by an increase in transmissibility at lower frequencies.

The acoustic power radiated by the foundation for the system with the original and the PDVA-enhanced isolators is calculated using Eq. (6) and compared on A-weighted decibel scale. Figs. 12(a) and (b) are for the cases where the DVA parameters are optimized within 200–3000 and 500–3000 Hz, respectively. It is clear that the DVA-enhanced isolator significantly reduces the noise radiation. At some frequencies (e.g. 2000 Hz in Fig. 12(a), and 1000 Hz in Fig. 12(b)), the acoustic power predicted for the case of the enhanced isolator can be up to 30 dB lower than that for the realistic isolator. As it was seen in Figs. 10 and 11 for the transmissibility, the DVA approach reduces the noise radiation above 500 Hz much more than it does in the frequency range of 200–500 Hz.

Table 3 compares the total acoustic power predicted for a system with the ideal (no inertia), the original, and the PDVA-enhanced isolators. It is seen that if the performance of the ideal massless isolator (row two) is considered as the base line, a theoretical noise reduction of 5.7 dB in the range of 200–3000 Hz and 11.2 dB in the range of 500–3000 Hz is obtainable by fully suppressing the IRs of the realistic isolator (third row). Using the DVA approach, the actual reduction is 2 and

Table 2
Isolator performance in terms of RMS transmissibility value of isolator 1

	Target frequency range for the performance evaluation (Hz)	
	200–3000	500–3000
System with ideal massless isolators	0.356	0.087
System with original isolators	0.59	0.444
System with DVA-enhanced isolator optimized for the transmissibility within 200–3000 Hz	0.63	N/A
System with DVA-enhanced isolator optimized for the transmissibility within 500–3000 Hz	N/A	0.044

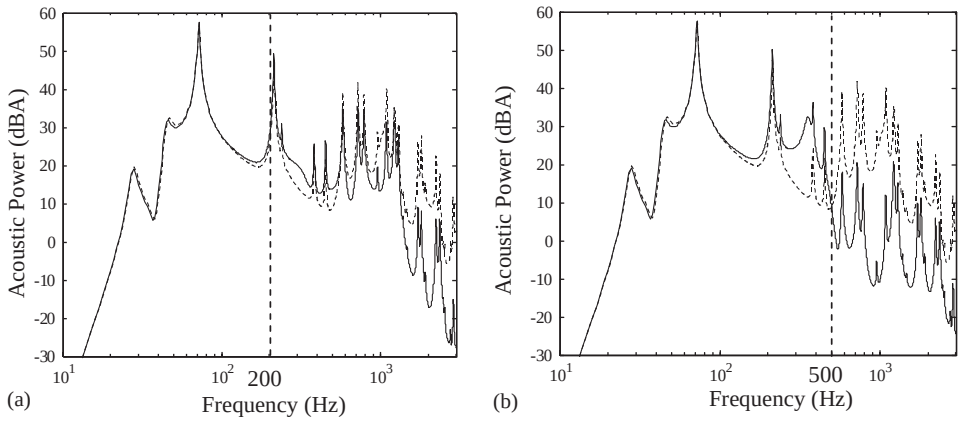

Fig. 12. Acoustic power radiated by the plate foundation when the system has PDVA-enhanced isolators and the DVA parameters are optimized within a frequency band of (a) 200–3000 Hz and (b) 500–3000 Hz: ——, PDVA-enhanced isolator; - - - -, original isolator.

Table 3
Isolator performance in terms of total acoustic power in dBA

	Target frequency range (Hz)	
	200–3000	500–3000
Ideal-massless isolator	47.9	41.2
Original isolator	53.6	52.4
DVA-enhanced isolator optimized for the transmissibility within 200–3000 Hz	51.7	N/A
DVA-enhanced isolator optimized for the transmissibility within 500–3000 Hz	N/A	31.8

20.6 dB for the above two frequency ranges, respectively. These results, once again, demonstrate that the PDVAs are very effective for improving the isolator's high frequency performance by suppressing the IRs. However, at low frequencies the passive DVA approach is not as effective as it is at high frequencies.

3.2. Desired control force for HDVA-enhanced isolator

Given the limitations of the PDVA-enhanced isolator at low frequencies revealed by the analytical model, the HDVA approach is expected to (a) effectively attenuate the transmitted force through the isolator at low frequencies, thus compensating the shortcoming of the PDVA-enhanced isolator, and (b) further improve the isolator performance at high frequencies. Since the practical effectiveness of the HDVA-enhanced isolator is largely determined by the control authority or capacity of the actual actuator, it is primarily investigated experimentally in this study. However, it is illustrative to estimate the control effort required by the HDVA configuration suggested in Section 2.2. An approach to quantify the control effort is by determining the *ideal* control force that will cancel the transmitted force to the foundation.

Though this "ideal" control force cannot be achieved in practice, it can (a) provide an indication of the expected level of control effort required at different frequencies, and (b) help determine the most effective frequency ranges in which the active control takes effect. Letting the transmitted force $F_B = 0$, the ideal control force, F_c, can be easily calculated from Eq. (7). As an example, the amplitude of the ideal control force normalized by F_0 is plotted in Fig. 13 (solid line). This result was obtained by substituting the parameters listed in Table 4 into Eq. (7). It should be pointed out that these parameters are estimated from the practical system that is used in the experimental validation.

From the results in Fig. 13, it is evident that the ideal control force is minimum at the two DVA tuning frequencies, i.e. 650 and 1060 Hz. The level of the control effort is nearly 30 dB (a factor of 31.6 in the amplitude) lower than the external load at these frequencies. Therefore, the DVA tuning frequencies are clearly identified by the appearance of two "valleys" on the curve of the ideal control force. The control effort away from these resonances increases. In particular, the control effort becomes larger than the disturbance force at low frequencies below 200 Hz. Thus, the performance of the active component will be largely determined by the actuator capabilities at low frequency, i.e. below the first PDVA resonance. As mentioned in the work by Burdisso and Heilmann [15], including a passive coupling element, i.e. spring–damper, in parallel with the active force is detrimental to the system because it leads to larger control forces for the same attenuation. For comparison, the ideal control force when there is passive coupling (i.e. damping and spring elements) between the two DVA masses is also shown in Fig. 13 (dashed line). It is seen that the passive coupling elements adversely increase the ideal control force at low frequencies which is the main target for the active component. Therefore, the passive elements should not be used in this application.

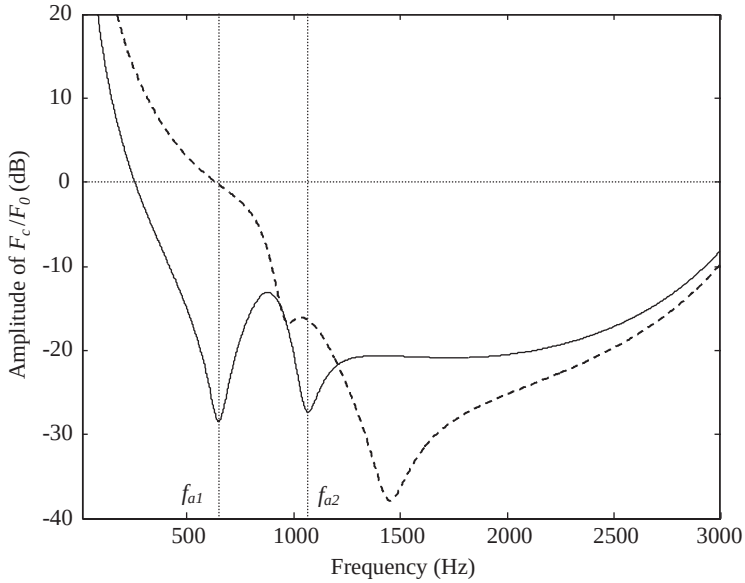

Fig. 13. Normalized ideal control force for a HDVA-enhanced isolator. The dashed curve (- - - - -) is for an isolator with passive elements coupling the DVA masses, while the continuous curve (———) is for an isolator without such elements.

Table 4
Parameters used to generate Fig. 13

Primary mass (kg)	$m = 1.0$
Intermediate mass (kg)	$m_{iu} = 0.154$, $m_{il} = 0.154$
Isolator parameters	
Density (kg/m^3)	1103
Length (m)	0.076
Young's modulus (MPa)	38.3
Loss factor	10%
DVA parameters	
Tuning frequency (Hz)	$f_{a1} = 1060$, $f_{a2} = 650$
Mass (kg)	$m_{a1} = 0.12$, $m_{a2} = 0.2$,
Loss factor	$\eta_{a1=8\%,}\ \eta_{a2} = 11\%$

4. Experimental validation

In this section, the IRs in a practical isolator are demonstrated and the performance of the proposed PDVA- and HDVA-enhanced isolators is investigated experimentally. For simplicity, all the experiments were based on a sdof system consisting of a primary mass connected to a foundation through a single isolator.

4.1. Prototype of the DVA-enhanced isolator

Two types of isolators were tested in the experiments. They are referred to as the *original* (without any DVA installed), and the *DVA-enhanced isolator*. Fig. 14 shows photographs of these two isolators. The original isolator is a commercial rubber mount manufactured by Lord Corporation. As indicated in the previous section, this original isolator is a regular, solid, isolator with no DVA attached to it. It has a diameter of 79.2 mm and a length of 76.2 mm. The density of the isolator material is 1103 kg/m^3. Two thin steel plates with 79.2 mm diameter are glued at both ends of the isolator; hence it is called *sandwich mount*. There is a threaded hole on the bottom plate and a stud on the top plate. Thus the isolator can be connected to other structures through the threaded hole and the stud. To incorporate DVAs into the isolator, another isolator was built using the same type of sandwich mount. This is a *hollow* isolator. There is a cylindrical cavity with diameter 45 mm in this isolator. The cavity is designed to house the two DVAs. Referring to Fig. 14(b), the hollow isolator consists of three segments with lengths $L_1 = L_3 = 20$ mm and $L_2 = 36$ mm. The length of L_1 or L_3 (20 mm) is roughly one-fourth of the isolator's total length (76 mm). This is in accordance with the suggestion from the previous analysis that the DVAs should be attached at the "one-quarter" position. Steel washers with mass 0.078 kg, acting as the IMs are attached at the end of each isolator segment. The two DVAs are embedded into the isolator through these steel washers. Each DVA mass is coupled to the isolator body through a plate spring that consists of several layers of metallic and viscoelastic materials. The plate spring has the same diameter as the isolator. The DVA damping is obtained mainly by means of the surface friction between the adjacent layers of the plate spring. The material, thickness and shape

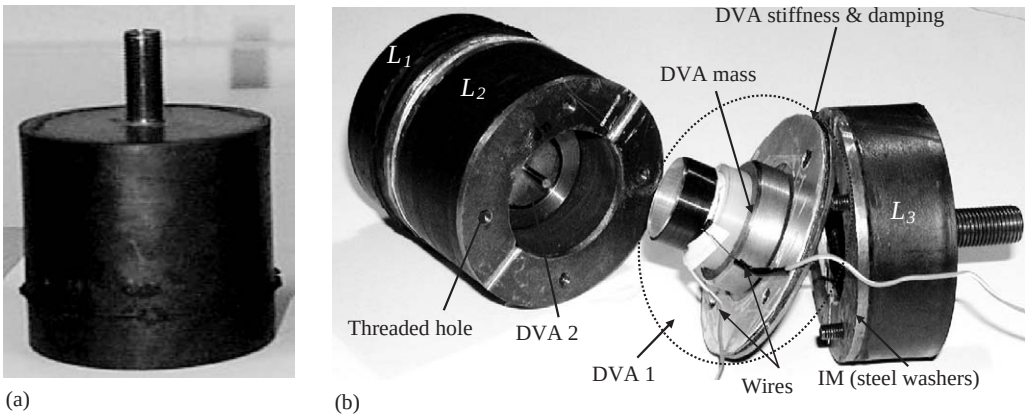

Fig. 14. Illustration of the (a) original isolator and (b) the assembly of the PDVA (controller off) or HDVA (controller on) enhanced isolator.

of each layer of the plate spring can be selected so as to achieve the desired damping and stiffness. A permanent magnet is attached to the mass of DVA2 and a voice coil is attached to the mass of DVA1. The positive and negative leads of the voice coil are connected to a signal amplifier and then to a controller (not shown in Fig. 14). This voice coil/magnet pair forms the actuator generating the active control force. When a current controlled by a controller passes through the coil, an electromagnetic force is developed between the coil and the magnet, and hence the two DVA masses. This active control force pair causes the masses to attract or repel, depending on the amplitude and polarity of the current. Through the way it is constructed, this prototype can act as either a PDVA- or a HDVA-enhanced isolator by simply turning the controller off and on.

4.2. Experimental setup

Fig. 15 shows the experimental setup which consists of a rigid primary mass connected to a foundation through a single isolator. The foundation can be either rigid or flexible. A rigid foundation is used when the intention of the experiment is to demonstrate the IRs in practical isolators, because in this case the interference of the foundation's dynamics is undesirable. However, a flexible foundation is used when showing the performance of the DVA-enhanced isolators, because it allows for the radiated acoustic power to be measured. In the latter case, the foundation is a simply supported rectangular aluminum plate with dimensions $0.71\,\mathrm{m} \times 0.508\,\mathrm{m}$ and 0.006 m thickness. The material density, Young's modulus, Poisson's ratio and loss factor of the plate material are $2700\,\mathrm{kg/m^3}$, $7.31 \times 10^{10}\,\mathrm{Pa}$, 0.33 and 1%, respectively. The primary mass is driven by an electromagnetic shaker whose output is white noise. Two force transducers are inserted between the shaker and the primary mass and between the isolator and the foundation to measure the input and the transmitted forces, respectively. The force transmissibility can then be obtained by feeding the two force signals into a spectrum analyzer. An array of 15 accelerometers mounted on the surface of the plate is used to measure the velocity distribution along the foundation. The distribution of this accelerometer array on the plate foundation is

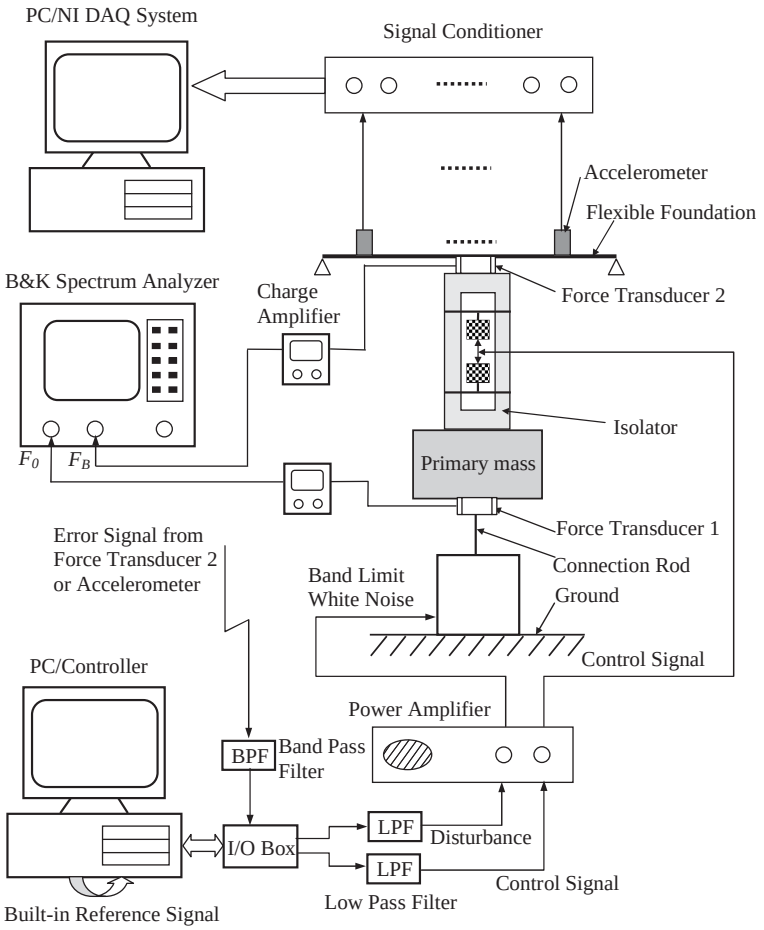

Fig. 15. Experimental setup.

shown in Fig. 16. The acoustic power radiated by the foundation is then estimated from this velocity information using Eq. (6) [19].

As it is mentioned earlier, the prototype shown in Fig. 14(b) can be used as either a PDVA- or a HDVA-enhanced isolator. The control approach adopted herein to adjust the active force in the HDVA-enhanced isolator is the Filtered-X least mean square (LMS) adaptive feedforward algorithm [20,21]. This algorithm requires a reference signal that is coherent with the disturbance. As it is indicated in Fig. 15 a disturbance signal, in the form of a white noise that is used to drive the shaker, was internally generated by the controller (the computer). This disturbance was also used as the internal reference signal. Therefore, the reference and the disturbance signals are perfectly coherent in the experiments. The built-in reference is filtered through a finite impulse response (FIR) control filter, i.e. the compensator, to generate the control signal. The weights of the FIR filter are updated by the LMS algorithm which seeks to minimize the signal from the error sensor. A detailed description of the Filtered-X control algorithm is beyond the scope of this

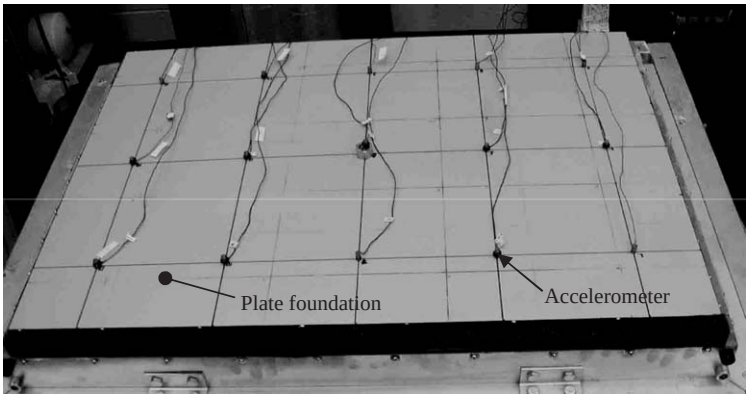

Fig. 16. The accelerometer array used to measure the foundation response.

paper and can be found in many Refs. [20,21]. Depending on the control objective, the error sensor could be the signal from the force transducer that measures the transmitted force, the response of the plate such as some weighted response of the accelerometer array, and the radiated sound measured using far-field microphones. The FIR filter has 256 coefficients. The sampling frequency of the controller is 5000 Hz. To assure a causal system, the disturbance signal generated by the controller and sent to the shaker is delayed by 64 time steps [22]. The disturbance and the control signals are low-pass filtered with a cutoff frequency of 1600 Hz. Since the main goal of the active control system is to operate in the isolation region, the error signal is band-pass filtered before it is fed back into the controller. The frequency control band considered in the experiments is from 200 to 1600 Hz. This frequency band approximately begins with the system resonant frequency of the mass-isolator-plate foundation vibration system shown in Fig. 15. To this end, it is important to mention that, when testing the HDVA-enhanced isolator, the key objective is to assess the potential of the additional active force in terms of the performance improvement. Thus, several practical factors in the implementation of an actual Filtered-X LMS control system are not addressed here. Issues such as finding a coherent reference signal for a practical feedforward implementation, delay effects in the control signal, control authority, need to be investigated in future endeavors.

4.3. Experimental results

4.3.1. Demonstration of the IRs in practical isolators

To demonstrate the IRs in a practical isolator and show their adverse effect on the isolator performance, the original isolator was tested using the setup shown in Fig. 15 where a rigid foundation consisting of a very massive steel plate was employed. The primary mass of the sdof system was 0.278 kg and the input disturbance was a band-limit white noise from 0 to 3200 Hz.

The dotted line in Fig. 17 is the experimental curve, which clearly shows, as expected, one system resonance at 424 Hz and the first two IRs at 1400 and 2230 Hz. The solid line in the same figure is the analytical prediction of the experimental case. This prediction was calculated using a sdof model that is simplified from the 3 dof reference model described in Section 2.3. Interested

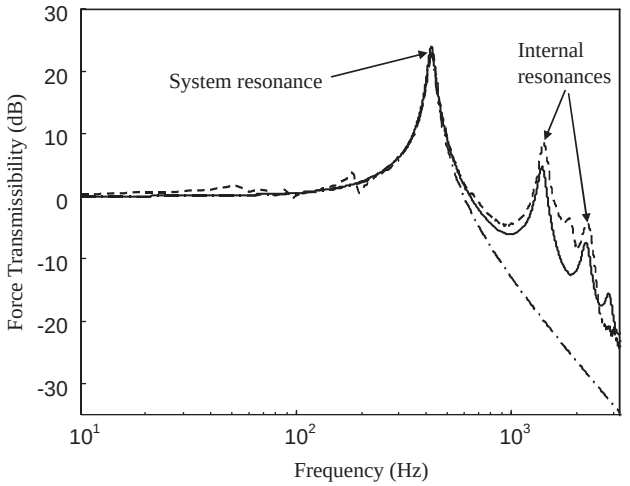

Fig. 17. Experimental demonstration of IRs in a commercial isolator and model validation: - - - -, experimental result for the original isolator; ———, analytical prediction for the original isolator; — · —, analytical prediction for the massless isolator.

readers should refer to Refs. [6,12] for detailed description regarding the simplification of the 3 dof system and the isolator model. It is seen that the analytical result agrees with the experimental data very well. Using this model, the transmissibility function can be also predicted for the ideal case where the isolator is assumed to be massless (dash–dotted line). Comparing the dash–dotted line to either the dotted or the solid line clearly shows that the true transmissibility of the practical isolator at the IR frequencies is at least 20 dB higher than that of the ideal one. This number is also an indication of the maximum obtainable attenuation by suppressing the IRs.

4.3.2. Performance validation of the DVA-enhanced isolator

After demonstrating the adverse effects of the IRs in a practical isolator, the effectiveness of the PDVA- and HDVA-enhanced isolators were experimentally investigated. The test setup is again the sdof system as shown in Fig. 15. However in this case, a flexible foundation in the form of a simply supported plate was used. Therefore, the radiated acoustic power from the foundation as well as the force transmissibility can be measured to evaluate the isolator performance. In the experiment, the primary mass was 1 kg and the excitation input to the shaker was a white noise in 0–1600 Hz frequency range. The experimentally estimated DVA parameters are listed in Table 5. Note that these parameters are the same as those listed in Table 4.

The experiments were arranged in such a way that (i) the PDVA-enhanced isolator was first tested by turning the control signal of the active force off; (ii) the HDVA-enhanced isolator was then examined by enabling the active force and (iii) the original isolator (shown in Fig. 14(a)) performance was measured by replacing the DVA-enhanced isolator with the original isolator. The effectiveness of the PDVA and HDVA approaches can be shown by comparing the results of the original isolator with those of the DVA-enhanced isolator. When testing the HDVA-enhanced isolator, the error signal is the transmitted force signal from force transducer 2 (Fig. 9). This error

Table 5
DVA parameters used in the prototype of DVA-enhanced isolator

	Mass (kg)	Loss factor (%)	Tuning frequency (Hz)
DVA 1	0.12	8	1060
DVA 2	0.2	11	650

signal was then fed into the LMS algorithm through a band-pass filter. The pass band range of this filter was determined in accordance to the designated working range, i.e. the isolation range of the isolator. To select the preferred isolation range of the experimental setup system, it is necessary to know its system resonant frequency. Because the stiffness of the aluminum plate foundation is relatively low, the shape of the transmissibility curve is significantly affected by the foundation's modes. Therefore, it is difficult to recognize the system resonance and the IRs from the experimental data. However, a numerical simulation shows that the system resonance of the experimental setup is around 200 Hz and the first two IRs are at frequencies higher than 500 Hz for the original isolator. Hence the frequency range of 200–1600 was used by the band-pass filter. In addition, since the isolation region of an isolator is usually defined as the frequency region that is at least $\sqrt{2}$ times higher than the system resonance frequency, the isolator performance as well as the DVA effectiveness was evaluated at frequencies higher than 300 Hz in the experiments.

Fig. 18 shows the force transmissibility across the original, the PDVA- and HDVA-enhanced isolators. Comparing to the transmissibility of the original isolator, it is seen that the PDVA-enhanced isolator significantly lowers the transmissibility at high frequencies, e.g. from 600 to 1600 Hz, but not in low frequencies. This observation is consistent with the conclusion obtained from the analytical model (Figs. 10 and 11) which showed that the PDVA approach is very effective in high frequency range where the IRs appear but less effective at low frequencies. On the other hand, when the feedforward controller is turned on (the solid line), the transmissibility level is significantly reduced in the whole isolation range from 300 to 1600 Hz. This result indicates that, in contrast to the PDVA approach, the HDVA approach is able to reduce the transmissibility of a regular isolator by as much as 20–30 dB at the lower end of the isolation range (e.g. <600 Hz in Fig. 18). In addition, the HDVA approach further improves the isolator performance at high frequencies (e.g. >600 Hz) by reducing the transmissibility of the PDVA-enhanced isolator to a lower level. The RMS transmissibility values in the 300–1600 Hz frequency band for the original isolator, the PDVA-enhanced isolator and the HDVA-enhanced isolator are 7.02, 5.76 and 0.55, respectively. Thus the PDVA approach reduced the overall transmissibility in the isolation region by 18.5%. When the HDVA is used, the RMS transmissibility is reduced to only 7.8% of that when the original isolator is used, which corresponds to an attenuation of 22.1 dB. This clearly demonstrates the effectiveness of the HDVA approach. The Filtered-X LMS feedforward control algorithm not only seeks to suppress the IRs but tries to reduce the response in the entire isolation range. Thus, it improves the isolator performance in a broadband sense.

An approach to further verify the effectiveness of the Filtered-X LMS algorithm is to compare the time domain error signals with and without control. To this end, this comparison is made in Fig. 19. The root-mean-square (rms) values of the error signals for these two cases are 0.1115 and 0.5763 V, respectively. This indicates that the controller successfully reduced the error signal by

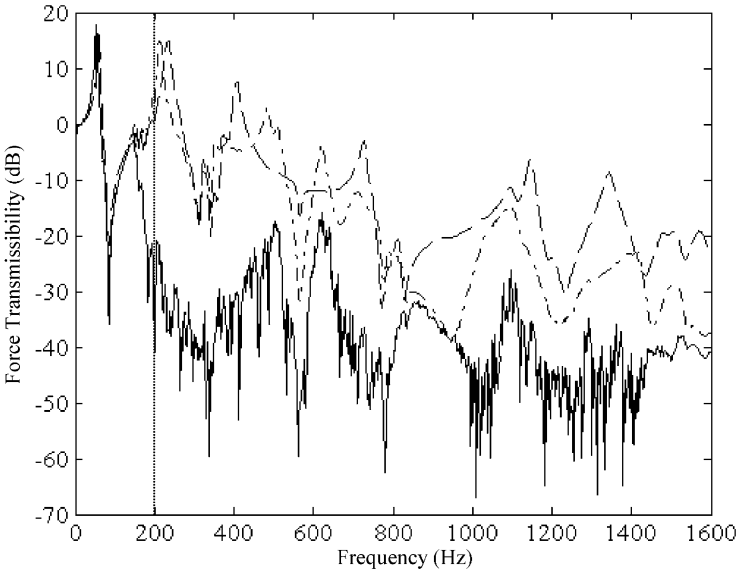

Fig. 18. Experimental force transmissibility. ———, HDVA-enhanced isolator; – · – · –, PDVA-enhanced isolator; – – – –, original isolator.

14.2 dB (or a factor of 5.1). For reference, the time history of the control signal is plotted in Fig. 19(c). Fig. 20 shows the spectrum of the control force. It is seen that, in the control band from 200 to 1600 Hz, the requirement for the control force is minimum around 600 and 950 Hz; away from these two frequencies, the amplitude of the control force increases. This experimental result is consistent with the analytical result shown in Fig. 13, which predicts two "valleys" around the tuning frequencies of the two DVAs, i.e. 650 and 1060 Hz. Note that, although the parameters used to generate the analytical curve are the same as those of the actual experimental system, the minimum control force does not occur at the same frequency on the experimental and the analytical curves. The experimental DVA tuning frequencies (the two "valleys") are lower than their analytical counterparts. One obvious reason leading to this discrepancy is that the analytical model assumed a rigid foundation while the experiment used a flexible foundation. Furthermore, the errors in estimating the parameters of the isolator and the DVAs could also contribute to this difference.

The acoustic power radiated by the flexible foundation was also experimentally estimated and shown in Fig. 21. To make the results comparable with each other, the acoustic power curves for the cases of the original isolator, the PDVA-enhanced isolator and the HDVA-enhanced isolator, were normalized by the amplitude of the input disturbance from the shaker. It is seen that compared to the original isolator significant noise reduction in the higher frequency band, i.e. >700 Hz, was achieved by the PDVA approach. In the low frequency range, the PDVA approach is not effective in reducing the radiated noise. This result is again consistent with the analytical prediction. However, by adding the active force, the HDVA approach (solid line in Fig. 21) considerably reduced the radiated acoustic power at low frequencies, thus complementing

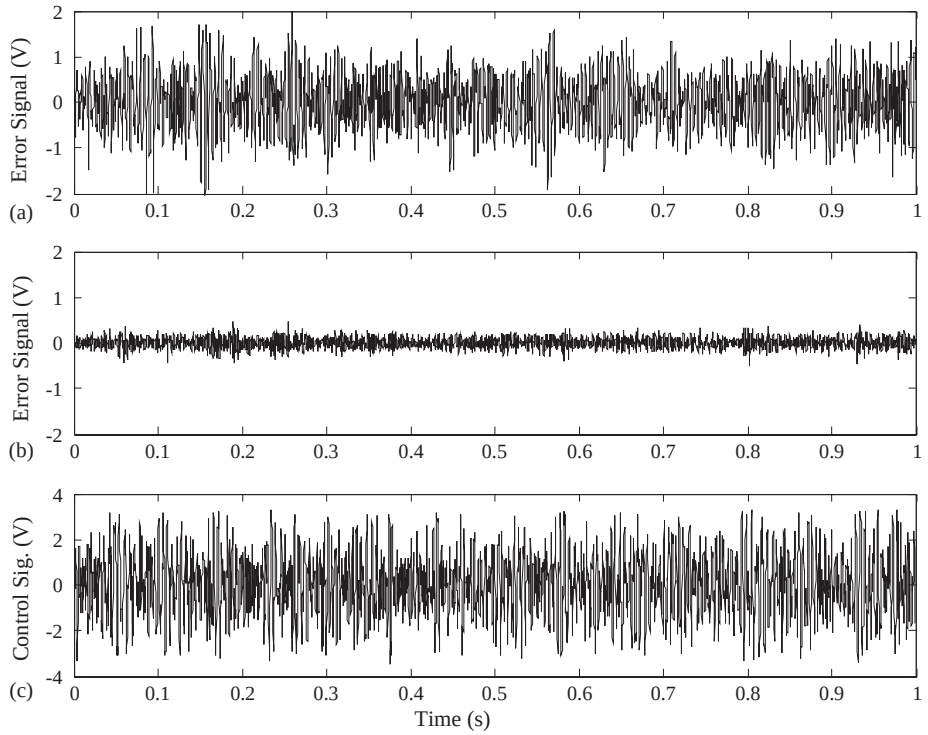

Fig. 19. Time history of the error signal when control is (a) off, (b) on, and (c) the control signal.

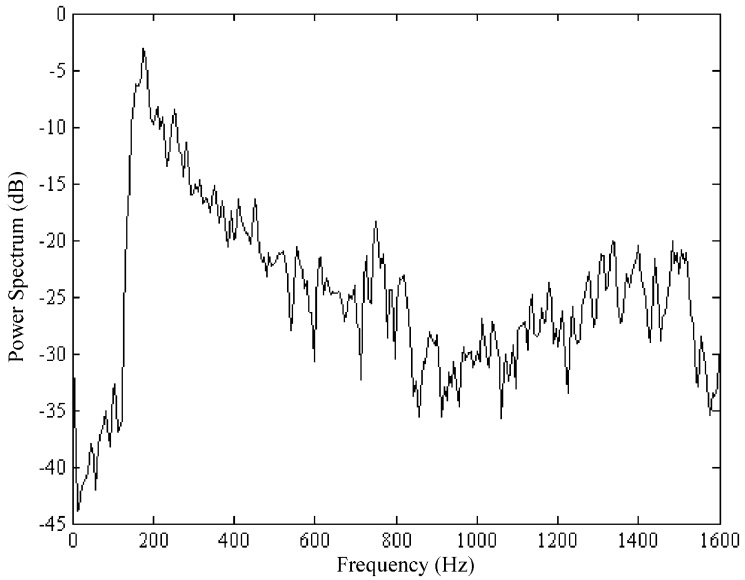

Fig. 20. Spectrum of the control force.

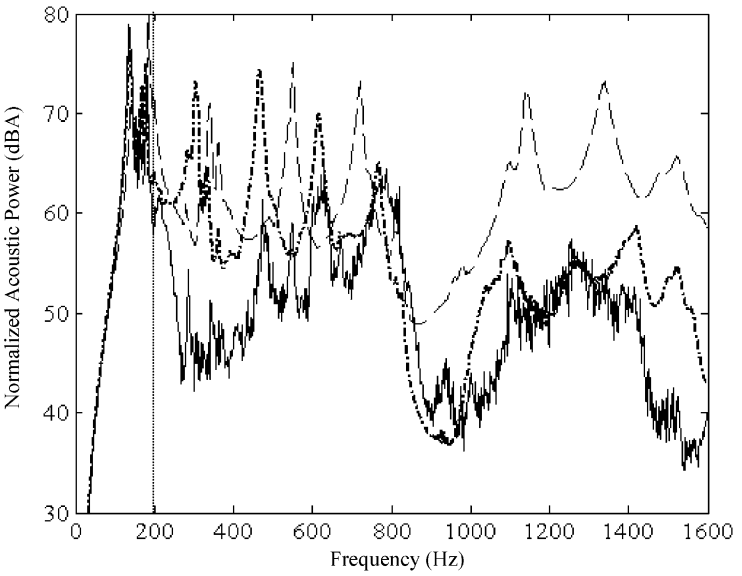

Fig. 21. Experimental acoustic power radiated by the foundation: ———, HDVA-enhanced isolator; — · —, PDVA-enhanced isolator; – – – –, original isolator.

the passive system effectively. In addition, the active system further improved the noise attenuation at high frequencies, although not as significantly as it did to the force transmissibility. The isolator performance can also be evaluated using the total A-weighted acoustic power within the desired isolation region, which was obtained by adding the contributions from the spectral lines in the 300–1600 Hz band. The total acoustic power for the cases of the original isolator, the PDVA-enhanced isolator and the HDVA-enhanced isolator is 94, 89.7 and 84.9 dBA, respectively. This indicates that an additional 4–9 dB noise attenuation can be obtained if the PDVA- or HDVA-enhanced isolator is employed instead of the original isolator. When comparing the cases of the PDVA-enhanced isolator and the HDVA-enhanced isolator in Figs. 18 and 21, it is interesting to note that a significant reduction in the transmitted force spectrum, due to the addition of the active force, did not translate in the same type of reduction in the acoustic power spectrum. For example, in the two frequency bands of 600–800 and 1100–1300 Hz, a large reduction in the force transmissibility was obtained when the HDVA approach was used (Fig. 18). However, in the same frequency ranges, the reduction in the noise radiation by the HDVA approach was trivial (Fig. 21). This difference may be due to the vibration modes of the plate foundation, which were not considered in this paper.

5. Discussion and conclusions

In this paper, the concept of using PDVA and HDVA to attenuate the IRs was studied. The novelty of the DVA application in this study is that the DVAs are embedded directly into the

isolator body. In the simulation model, two DVAs were employed which were attached to an isolator at two positions with distances equal to one-quarter and three-quarters of the isolator length measured from either end of the isolator. The effectiveness of the PDVA approach was assessed using a 3 dof reference model. At least a 10 dB reduction in the force transmissibility was observed around the IR frequencies. The PDVA approach also resulted in a 2 and 20.6 dB reduction in sound power radiation in the 200–3000 and 500–3000 Hz frequency bands, respectively. The ideal control force required by the HDVA approach was analyzed using a mathematical model. This analysis evaluates the effectiveness of the active control force at different frequencies.

To verify the importance of the IRs in practical isolators, a commercial rubber mount was tested. The experimental transmissibility curve shows similar behavior as that predicted by the analytical model. This result clearly demonstrated that the IR is a practical problem that degrades the isolator performance. To experimentally validate the effectiveness of the proposed approach of using DVAs to suppress the IRs, a DVA-enhanced isolator prototype, which can be configured as either a PDVA approach or a HDVA approach, was built and tested. It has been observed that the PDVA-enhanced isolator significantly reduces both the force transmissibility and the radiated acoustic power. Experimental data showed that an enhanced isolator with PDVAs has force transmissibility up to 20 dB lower than that of the original isolator without DVAs. A reduction of 4.3 dB for the total acoustic power within the isolation range (i.e. 300–1600 Hz) is achieved by using PDVAs. Although both the analytical and the experimental results have shown that the PDVA approach is effective in improving the isolator performance by attenuating the IRs, especially at high frequencies, these results also showed that the PDVA approach did not result in satisfactory improvement at low frequencies, i.e. the frequency range below the IR frequencies. In some cases, the PDVA-enhanced isolator performed worse than the original isolator at low frequencies. This is because the PDVA as well as the IMs induce new resonances at the low frequency region. The HDVA approach is a good candidate to compensate the limitation of the PDVA approach.

By adding an active force in the PDVA configuration, the performance of the HDVA-enhanced isolator was tested. The active force was implemented by means of a voice coil–magnet pair. The adaptive Filtered-X LMS feedforward control algorithm was chosen to control the active force in the experiments. This algorithm seeks to minimize the error signal by adapting the coefficients of a FIR control filter. The error signal used in the feedforward control experiments was the transmitted force through the isolator. It was observed that the HDVA approach improved performance substantially over the PDVA approach at low frequencies. The hybrid approach further enhanced the isolator performance obtained by the PDVA approach at high frequencies, thus offering a significant broadband improvement. Comparing to the performance of the original isolator that does not have DVAs, the RMS transmissibility and total acoustic power in the isolation region were reduced by 92.2% and 9.1 dB, respectively, by using the HDVA approach. These numbers are much higher than their counterparts for the PDVA approach. It should be mentioned that, if the primary control goal is to reduce the noise radiated by the foundation, the transmitted force used in the previous experiments is not the best error signal since it is not a direct metric for noise radiation. Hence, better noise reduction would be expected if a signal from an acoustic transducer (e.g. a microphone) were directly used as the error signal in the HDVA approach.

Acknowledgements

The study presented in this paper was partially supported by an unrestricted grant of the University Research Program of Ford Motor Company. The authors are thankful to Dr. Everett Kuo for serving as the technical liaison between Virginia Tech, The University of Toledo and Ford Motor Company.

References

[1] M. Harrison, A.O. Sykes, M. Martin, Wave effects in isolation mounts, *Journal of the Acoustical Society of America* 24 (1952) 62–71.
[2] J.C. Snowdon, Vibration isolation: use and characterization, *Journal of the Acoustical Society of America* 66 (1979) 1245–1274.
[3] L. Kari, Dynamic transfer stiffness measurements of vibration isolators in the audible frequency range, *Journal of Noise Control Engineering* 49 (2) (2001) 88–102.
[4] E.E. Ungar, C.W. Dietrich, High-frequency vibration isolation, *Journal of Sound and Vibration* 4 (1966) 224–241.
[5] Y. Du, R. Burdisso, E. Nikolaidis, D. Tiwari, E. Y. Kuo, Internal resonances in vibration isolators and their suppression using dynamic vibration absorbers, *Inter-Noise 2002*, Dearborn, MI, USA, August 19–21, 2002.
[6] Y. Du, R. Burdisso, E. Nikolaidis, D. Tiwari, Effects of isolators internal resonances on force transmissibility and radiated noise, *Journal of Sound and Vibration* 268 (4) (2003) 751–778.
[7] G.R. Tomlinson, *Vibration Isolation in the Low and High Frequency Range*, Mechanical Engineering Publication, Edmunds, Suffolk, England, 1982 pp. 21–29.
[8] J.C. Snowdon, Isolation from vibration with a mounting utilizing low- and high-damping rubberlike materials, *Journal of the Acoustical Society of America* 34 (1962) 54–61.
[9] J.C. Snowdon, *Vibration and Shock in Damped Mechanical Systems*, Wiley, New York, 1968.
[10] J.C. Snowdon, Compound mounting systems that incorporate dynamic vibration absorbers, *Journal of Engineering for Industry*, November (1975) 1204–1211.
[11] V.H. Neubert, Dynamic absorbers applied to a bar that has solid damping, *Journal of the Acoustical Society of America* 36 (4) (1964) 673–680.
[12] Y. Du, Internal Resonances in Vibration Isolators and their Control using and Hybrid Dynamic Vibration Absorbers, PhD Thesis, Virginia Tech, 2003.
[13] A.E. Love, *A Treatise on the Mathematical Theory of Elasticity*, Dover, New York, 1944.
[14] J.Q. Sun, M.R. Jolly, M.A. Norris, Passive, adaptive and active tuned vibration absorbers—a survey, *Transactions of the ASME* 117 (1995) 234–242.
[15] R.A. Burdisso, J.D. Heilmann, A new dual-reaction mass dynamic vibration absorber actuator for active vibration control, *Journal of Sound and Vibration* 214 (5) (1998) 817–831.
[16] A.O. Sykes, Isolation of vibration when machine and foundation are resilient and when wave effects occur in the mount, *Noise Control* (1960) 115–130.
[17] L. Cremer, M. Heckl, E.E. Ungar, *Structure-borne Sound*, Springer, Berlin, 1987.
[18] D. Tiwari, Design Optimization of Enhanced Isolators for Suppression of Internal Resonances, Master Thesis, Mechanical Industrial and Manufacturing Engineering, The University of Toledo, 2003.
[19] S.J. Elliott, M.E. Jonson, Radiated modes and the active control of sound power, *Journal of the Acoustical Society of America* 94 (1993) 2194–2204.
[20] S.M. Kuo, D.R. Morgan, *Active Noise Control Systems—Algorithms and DSP Implementations*, Wiley, New York, 1996.
[21] J.S. Vipperman, R.A. Burdisso, C.R. Fuller, Active control of broadband structural vibration using the LMS adaptive algorithm, *Journal of Sound and Vibration* 166 (2) (1993) 283–299.
[22] R.A. Burdisso, J.S. Vipperman, C.R. Fuller, Causality analysis of feedforward-controlled systems with broadband inputs, *Journal of the Acoustical Society of America* 94 (1) (1993) 234–242.